

# UC San Diego

## UC San Diego Previously Published Works

### Title

Clinical Phenotype of Musladin-Lueke Syndrome in 2 Beagles.

### Permalink

<https://escholarship.org/uc/item/0573t252>

### Journal

Journal of Veterinary Internal Medicine, 31(2)

### Authors

Packer, R

Logan, M

Guo, L

et al.

### Publication Date

2017-03-01

### DOI

10.1111/jvim.14654

Peer reviewed

## Case Report

*J Vet Intern Med* 2017;31:532–538

## Clinical Phenotype of Musladin-Lueke Syndrome in 2 Beagles

R.A. Packer, M.A. Logan, L.T. Guo, S.S. Apte, H. Bader, D.P. O'Brien, G. Johnson, and G.D. Shelton

Musladin-Lueke syndrome (MLS), previously termed Chinese Beagle syndrome, is an autosomal-recessive connective tissue disorder characterized by extensive fibrosis of the skin and joints that was first identified in Beagles in the 1970s. Recent research identified a founder mutation (c.660C>T; p.R221C) in the *ADAMTSL2* gene in Beagles with MLS. Here, we report the detailed clinical phenotype and laboratory findings in 2 Beagles affected with MLS. We discuss these findings in relation to the human disorder geleophysic dysplasia (GD), which also arises from recessive *ADAMTSL2* mutations, and recent findings in *Adamtsl2*-deficient mice.

**Key words:** ADAMTSL2; ballerina Beagle syndrome; Chinese Beagle syndrome; geleophysic dysplasia; canine.

## Case 1

A 4-year-old, female spayed Beagle was referred for a history of gait abnormalities (present since birth), intermittent urinary incontinence, and generalized seizures which were present since 2 years of age and had been treated by administration of phenobarbital. The dog appeared to walk on the digits (“tiptoes”) with all 4 limbs in rigid extension during ambulation (Fig 1A). Tail carriage was low, and tail tone was rigid. Physical examination revealed a broad skull with wide-set eyes (Fig 1A), characteristic ridge within the ear cartilage (Fig 1B), brachydactyly of the outer toes, pronounced skeletal muscle definition, mild bilateral carpal valgus deformity, decreased to absent range of motion in joints of all 4 limbs, and a grade II/VI intermittent left basilar systolic murmur. There were no other abnormalities on the remainder of the physical or fundoscopic examination. No other abnormalities apart from the gait and tail abnormalities were detected on neurologic examination, although flexor withdrawal reflexes were difficult to evaluate due to decreased range of motion.

CBC revealed panleukopenia ( $2.99 \times 10^3/\mu\text{L}$ , reference range  $6\text{--}17 \times 10^3/\mu\text{L}$ ), mature neutropenia

## Abbreviations:

BAEP/BAER	brainstem auditory-evoked potentials/responses
CSF	cerebrospinal fluid
ECG	electrocardiograph
ECM	extracellular matrix
EMG	electromyography/electromyogram
GD	geleophysic dysplasia
MLS	Musladin-Lueke syndrome
MNCV	motor nerve conduction velocity
MRI	magnetic resonance imaging
RNS	repetitive nerve stimulation
SMA	$\alpha$ -smooth-muscle actin
SMC	smooth-muscle cells

( $2.24 \times 10^3/\mu\text{L}$ , reference range  $3\text{--}12 \times 10^3/\mu\text{L}$ ), lymphopenia ( $0.54 \times 10^3/\mu\text{L}$ , reference range  $1\text{--}5 \times 10^3/\mu\text{L}$ ), and eosinopenia ( $0.03 \times 10^3/\mu\text{L}$ , reference range  $0.1\text{--}1.25 \times 10^3/\mu\text{L}$ ).

A repeat CBC performed 2 weeks later and after gradual discontinuation of phenobarbital revealed resolution of the pancytopenia. Abnormalities were not detected on abdominal radiographs. The thoracic radiographs revealed a vertebral heart score of 12.25 (reference range  $8.7\text{--}10.7$ )<sup>1</sup> with no cardiopulmonary changes noted. The ECG revealed a sinus arrhythmia with a mean electrical axis of +30 and one of the criteria for left ventricular enlargement ( $R > 1.0$  in lead I). The echocardiogram revealed turbulent flow across both the left and right ventricular outflow tracts, but no valvular changes, wall thickening, or chamber dilatation were identified.

Joint range of motion remained restricted under general anesthesia. No abnormalities were identified with MRI. CSF analysis showed that nucleated cell counts and protein concentration were within reference range, with vacuolated mononuclear cells suggestive of lipid/myelin phagocytosis. Electromyography (EMG) of the palmar and plantar interossei, flexor carpi ulnaris, extensor carpi radialis, biceps, triceps, supraspinatus, infraspinatus, lateral gastrocnemius, medial gastrocnemius, cranial tibialis, biceps femoris, vastus lateralis, semimembranosus, semitendinosus, and tail muscles revealed mildly increased insertional activity in several muscle groups (palmar and plantar interossei, flexor

From the Department of Veterinary Clinical Sciences, Purdue University, West Lafayette, IN (Packer, Logan); Department of Basic Medical Sciences, Purdue University, West Lafayette, IN (Packer, Logan); Department of Pathology, School of Medicine, University of California - San Diego, La Jolla, CA (Guo, Shelton); Department of Biomedical Engineering, Cleveland Clinic Lerner Research Institute, Cleveland, OH (Apte, Bader); Department of Veterinary Medicine and Surgery, University of Missouri, Columbia, MO (O'Brien, Johnson).

Corresponding author: Dr. R.A. Packer, Department of Clinical Sciences, Colorado State University, College of Veterinary Medicine and Biomedical Sciences, 300 W Drake Road, Fort Collins, CO 80523; e-mail: Rebecca.Packer@colostate.edu.

Submitted July 17, 2016; Revised October 18, 2016; Accepted December 8, 2016.

Copyright © 2017 The Authors. Journal of Veterinary Internal Medicine published by Wiley Periodicals, Inc. on behalf of the American College of Veterinary Internal Medicine.

This is an open access article under the terms of the Creative Commons Attribution-NonCommercial License, which permits use, distribution and reproduction in any medium, provided the original work is properly cited and is not used for commercial purposes.

DOI: 10.1111/jvim.14654

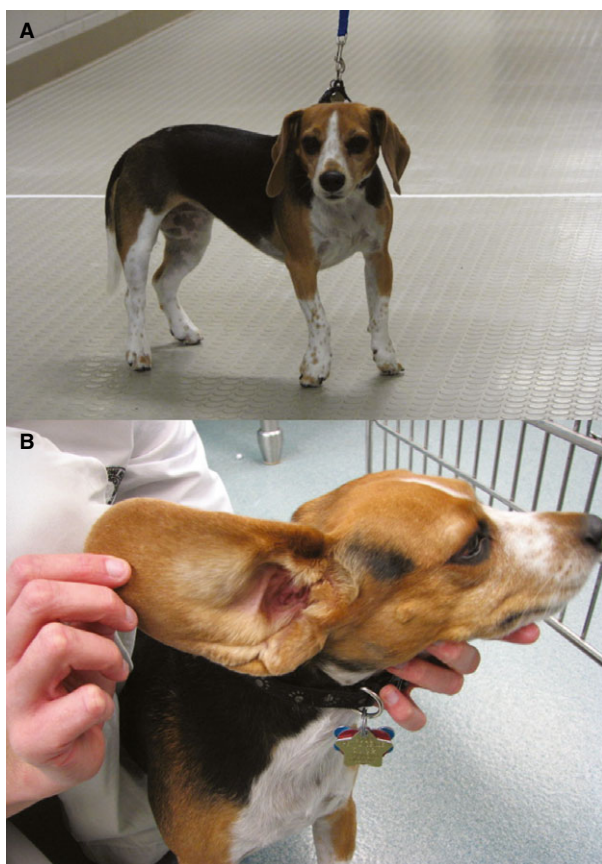


**Fig 1.** Image of Case 1 illustrating the “tiptoe” posture and characteristic facial features (A), and folded ear (B). Characteristic facial features include a broad muzzle and wide-set eyes.

carpi ulnaris, semimembranosus, semitendinosus, and tail), but no spontaneous activity was identified. Due to the sporadic nature of the findings and lack of consistent nerve distribution patterns, the increased insertional activity was most likely not clinically relevant. Motor nerve conduction velocity of the tibial nerve was within the reference range.

Biopsies were obtained from the cranial tibial muscle and either flash-frozen in isopentane precooled in liquid nitrogen or fixed in 10% neutral-buffered formalin and paraffin-embedded. No abnormalities were identified that would suggest a congenital myopathy or muscular dystrophy. Compared to an age-matched control, no expansion of endomysial or perimysial connective tissues was found, and localization of these proteins was appropriate, based on cryosections incubated with monoclonal or polyclonal antibodies against collagen VI and laminin  $\alpha$ -2 (gifts from Eva Engvall); and fibrillin-1 (polyclonal antibody 9543), fibrillin-2 (polyclonal antibody 868), and fibrillin-3 (monoclonal antibody 689, gifts from Lynn Sakai). Stainings also included antibodies against dystrophin (DYS1), utrophin (NCL-DRP2), and developmental myosin heavy chain (dMHC) (all from Novocastra Laboratories; Leica Biosystems Inc, Buffalo Grove, IL), and  $\alpha$ -sarcoglycan (gift from Eva Engvall).

Results of tests for organic acid and amino acid analysis (Biochemical Genetics Laboratory, University of California San Diego, LaJolla, CA), carbohydrate screening, and a mucopolysaccharide spot test (Penn-Gen Laboratory, University of Pennsylvania, Philadelphia, PA) in urine were negative.

## Case 2

An 11-week-old, male Beagle puppy was referred for difficulty righting and stiff gait. The pup was among a litter of 6, 2 of which died at 1 day of age. Of the remaining 4 puppies (2 males and 2 females), this was the only affected puppy. This litter was the first for the pairing of bitch and sire. The breeders did not notice any abnormalities until the puppy was 9 weeks of age, at which time he began having trouble righting himself and appeared stiff. The stiffness was progressive with concurrent development of characteristic facial features, including broad skull and wide-set eyes. The disposition of the affected pup was purportedly very placid compared to unaffected littermates.

On physical examination, the puppy had thick skin, a broad muzzle, and wide-set eyes. Musculature felt unusually dense on palpation. He had a stiff gait and walked on the digits. The limbs were rigid and could not be flexed even under sedation. Other than altered gait, no abnormalities were found on neurologic examination. Diagnostic examinations included electrophysiologic evaluation (EMG, MNCV of the tibial nerve, repetitive nerve stimulation, and brainstem auditory-evoked potentials (BAEP)), all of which were within reference ranges. The puppy presented for suspicion of Musladin-Lueke syndrome. The puppy was euthanized and submitted for postmortem examination.

Muscle histopathology and immunohistochemistry for Case 2 were similar to Case 1. On postmortem examination of Case 2, lesions were consistent with widespread accumulation of collagen. Skin was diffusely thickened with extensive fibrosis of the hypodermis and adhesion to underlying layers. Collagen and connective tissue surrounding kidney, adrenal glands, lymph node capsule, small intestine, esophagus, testes, trachea, pinnae, stomach, urinary bladder, heart, and dura was dense. Staining with picrosirius red showed birefringent red/green fibers characteristic of collagen in vessel walls and interstitium of organs. Elastin was well represented. The epimysium surrounding some entire muscles was excessive and comprised of dense collagen (not shown), and in some cases, it was restrictive; however, perimysial and endomysial connective tissue between muscle fascicles and individual myofibers, respectively, appeared normal (Fig 2). Muscle bundles contained almost no fat (appropriate for age), and the epimysial connective tissue was a dense seam of tissue containing blood vessels. Ligaments and, to a lesser extent, tendons diffusely contained an increase in tenocyte nuclei, and there were small foci of mineralized mucinous matrix (sections with ligamentum nuchae were especially affected). Nerve fibers in the sciatic nerve were surrounded by visible, but not excessive, endoneurium.

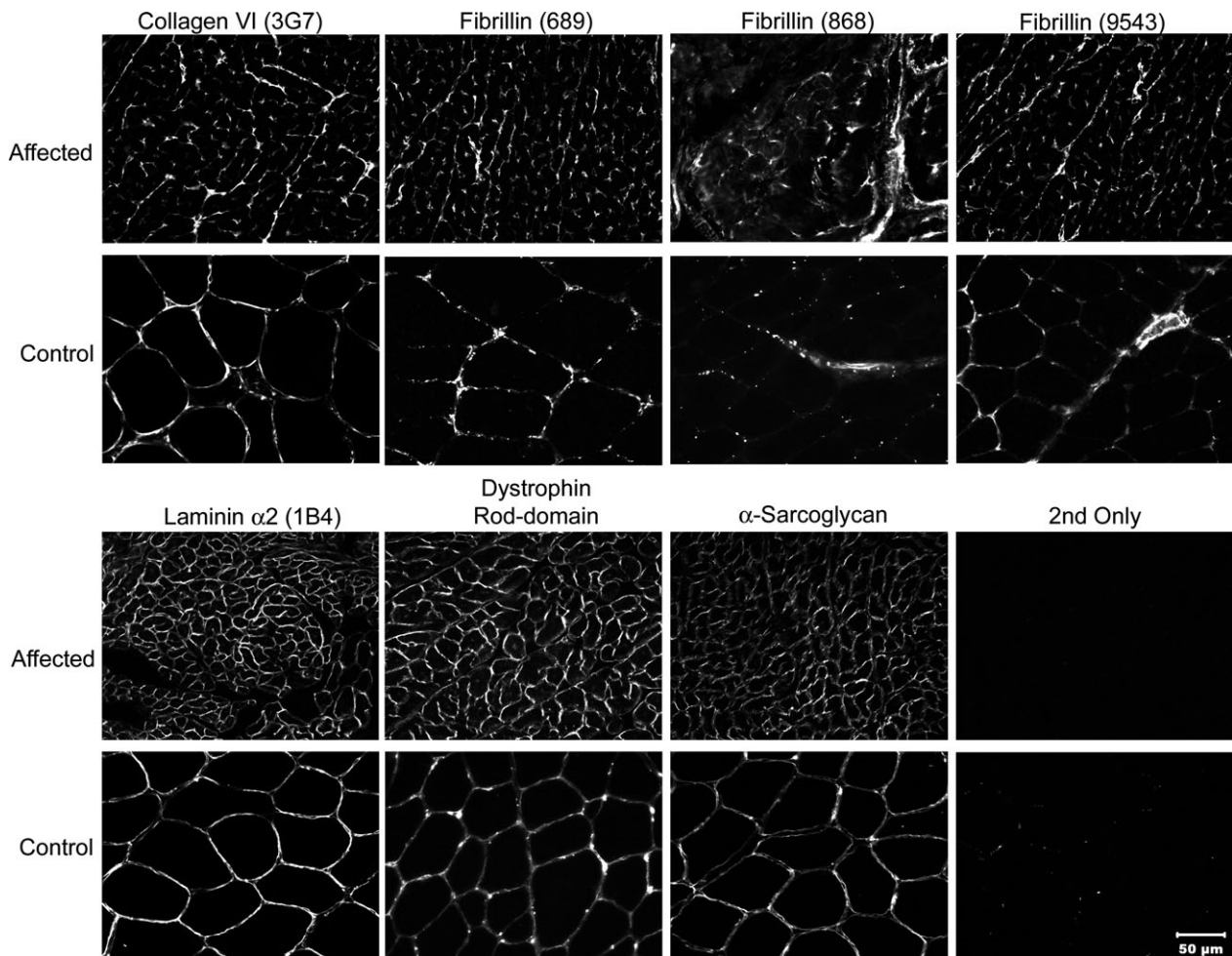


**Fig 2.** Immunofluorescence staining of muscle cryosections from a Beagle dog with Musladin-Lueke syndrome (Case 2) and age-matched but not breed-matched control muscle. Staining was performed for localization of laminin  $\alpha 2$ , the rod domain of dystrophin, utrophin,  $\alpha$ -sarcoglycan, collagen VI, fibrillins, and developmental myosin heavy chain. The endomysial (surrounding individual muscle fibers) and perimysial connective tissue layers (surrounding muscle fascicles) did not differ from control muscle. Regenerating fibers were not observed with the antibody against developmental myosin heavy chain. In the figure, fibrillin 9543 binds to fibrillin 1, fibrillin 868 binds to fibrillin 2, and fibrillin 689 binds to fibrillins 1, 2, and 3. All images photographed at the same magnification. Bar = 50  $\mu$ m for all images.

Acute myocardial degeneration and necrosis was present. Much of the cortical bone appeared sclerotic, with densely fibrous periosteum. Several focal areas of replacement of cortical bone with fibrous tissue were present in the digit (P2), rib, and ulna. The calvarial and facial bones were thickened. The dura was tougher and more opaque than expected for the age. A region of the central cartilage of the pinnae was thickened in a vertical line (similar to Fig 1B). The joint surfaces appeared normal on gross examination. Abnormalities were not detected in other organs, including the brain and peripheral pulmonary airways.

Both cases were homozygous for a founder mutation in the *ADAMTSL2* gene on CFA 9, indicative of Musladin-Lueke syndrome, as previously reported.<sup>2</sup>

Further characterization of fibroblasts was performed to evaluate the functional effects of Musladin-Lueke syndrome on tissues. Dermal fibroblasts from both cases were cultured from skin biopsies. Skin samples

were minced and plated, allowing cells to adhere to tissue culture plates (MLS 1, 2; control 1, 2), or tissue was further enzymatically dissociated (controls 3, 4, 5) using 0.1% collagenase (CLS4, Worthington Biochemical Corporation) and 0.05% elastase (Worthington Biochemical Corporation). As MLS fibroblasts grew slower than fibroblasts from control dogs, they were plated at higher density to ensure that control and MLS fibroblasts reached confluency at the same time. After reaching confluency, cells were cultured for another 2 days in 10% FBS to allow matrix synthesis and were incubated for 2 days in serum-free media. Subsequently, their conditioned medium was used to assess TGF $\beta$  secretion, and cellular smooth-muscle actin (SMA) expression was assessed by immunofluorescence. The total TGF $\beta$  in medium was measured by ELISA (Promega) in triplicate, and the TGF $\beta$  reading was conducted immediately after obtaining primary cell lines. High TGF $\beta$  levels were detected in media from the MLS fibroblasts (Case



2), whereas no free TGF $\beta$  was detected in the wild-type sample (control dog 1 (Ctl1)) (Fig 3A). Dermal fibroblasts from Case 2 and from 4 control adult dogs of unknown genetic background (Ctl1, Ctl3, Ctl4, Ctl5) were stained with anti- $\alpha$  SMA antibody (clone 1A4, Sigma 2547; diluted 1/400) and analyzed by flow cytometry. Fibroblasts from Case 1 and control dog 2 (Ctl2) were not included in the flow cytometry analysis due to a lack of sufficient cells. Whereas fibroblasts from 3 of the control dogs (Ctl1, Ctl3, Ctl5) expressed only low levels of SMA, and fibroblasts from control dog 4 showed both low and high expressing populations, MLS fibroblasts (Case 2) showed uniformly high SMA expression approaching that of smooth-muscle cells (SMC) (Fig 3B). SMA expression was also

assessed by immunofluorescence staining<sup>3</sup> and confirmed high SMA expression in MLS fibroblasts (Case 2) (Fig 3C). In addition, by immunofluorescence, MLS fibroblasts from Case 1 were also found to express high levels of SMA (Fig 3D). To test contractility,  $3 \times 10^4$  skin fibroblasts from Case 2 and 5 control dogs (Ctl1 through Ctl5) were seeded into collagen gels, and each sample was assayed in triplicate for the extent of contraction, as previously described.<sup>3</sup> MLS fibroblasts showed significantly enhanced contractility (Fig 4A,B). To assess whether there was a correlation between SMA expression and contractility, whole-mount SMA staining of contracted collagen gels was performed, which also showed strong SMA staining in the MLS cells (Fig 4C).

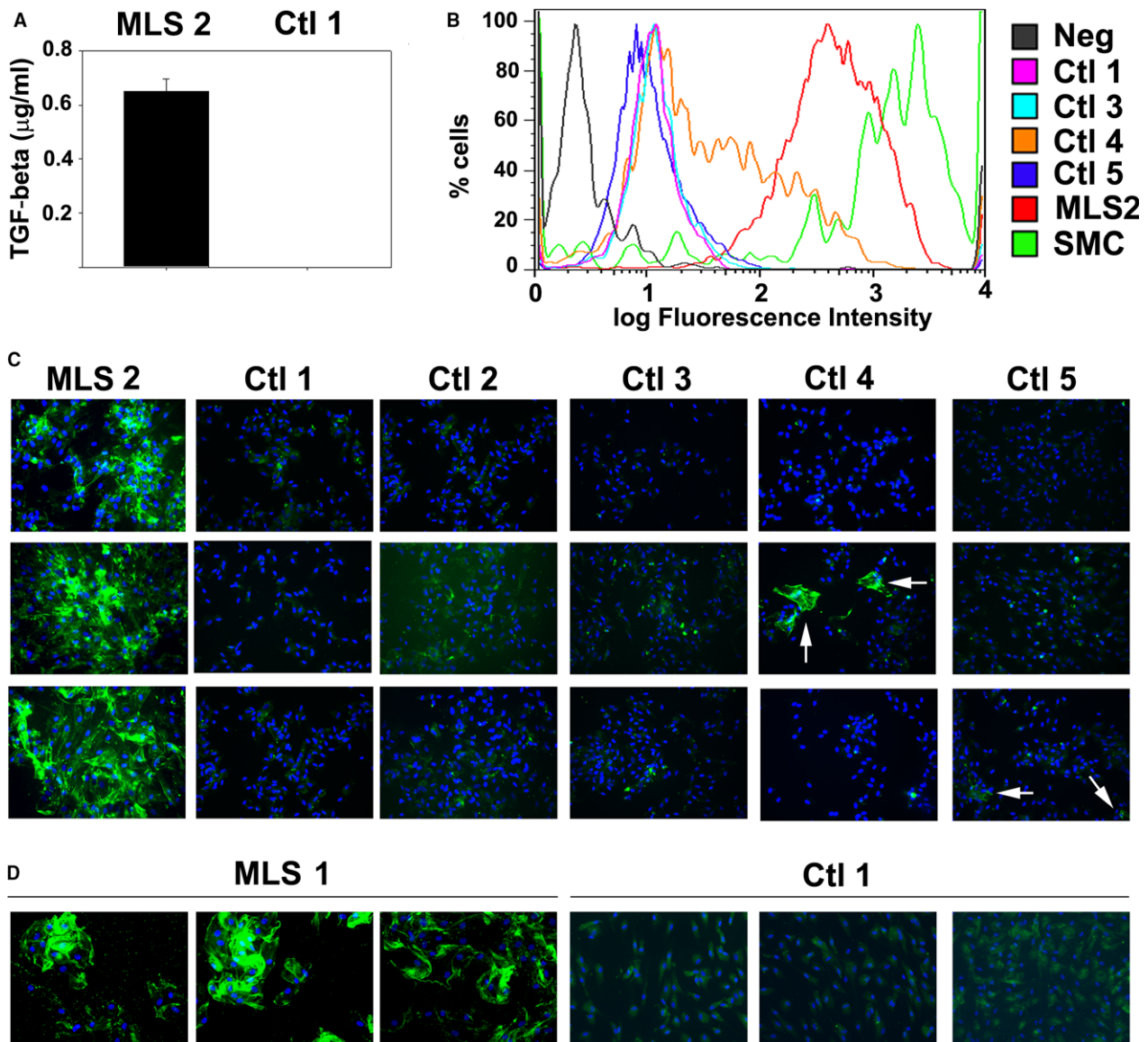


**Fig 3.** Skin fibroblasts from MLS dogs (MLS 1, Case 1; MLS 2, Case 2) exhibit characteristics of myofibroblasts. MLS fibroblasts secrete high levels of TGF $\beta$  (A) and express the myofibroblast marker  $\alpha$ -smooth-muscle actin determined by (B) flow cytometry and (C, D) immunofluorescence (SMA, green nuclei; DAPI, blue nuclei). Only few SMA-positive cells were observed in controls (arrows).

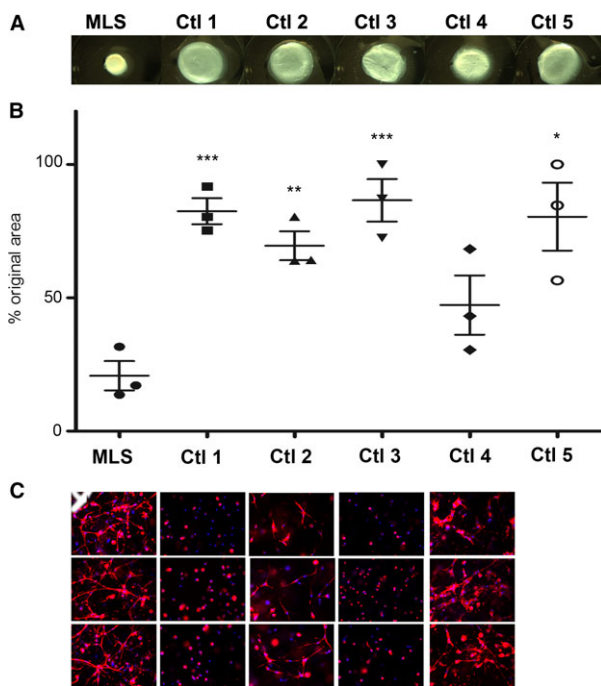


**Fig 4.** MLS cells contract collagen gels more efficiently than fibroblasts from control dogs (MLS 2, Case 2). Shown are representative images of gels after contraction (A), and the percentage of the original surface area after contraction (mean  $\pm$  SEM of 3 independent experiments) (B). The significance of the difference between the MLS and control samples was determined with a Student's *t*-test (tails 2, type 1), and the *P* values were found to be  $<.05$  (\*),  $<.01$  (\*\*), and  $<.0003$  (\*\*\*). The difference between MLS and Ctl 4 was not significant. SMA fluorescence of cells in contracted collagen gels (nuclei are stained blue using DAPI) shows comparable cell density but stronger SMA staining and extended morphology of MLS cells (C).

## Discussion

A variety of mutations affecting different regions of the *ADAMTSL2* gene (including the p.R221C substitution identified in MLS) in humans leads to a severe connective tissue disorder, autosomal-recessive geleophysic dysplasia (GD) type 1.<sup>4,5</sup> *ADAMTSL2* interacts with the microfibril-forming extracellular matrix (ECM) glycoproteins fibrillin-1 and fibrillin-2, as well as with latent TGF- $\beta$  binding protein 1 (LTBP1).<sup>4,6,7</sup> Dominant GD is caused by mutations affecting *FBNI*,<sup>6</sup> and a fibrillin-1 defect in mice (*Tight skin (Tsk)*) also results in severe fibrosis.<sup>2,8</sup> Tight skin, however, has not been observed in *Adamtsl2*<sup>-/-</sup> mice, which die at birth with severe bronchial occlusion. This and additional differences among GD, MLS, and mouse *Adamtsl2* knockouts are discussed.<sup>7,9,10</sup> Because of the established role of fibrillin microfibrils and LTBP1 in sequestering and maintaining the latency of TGF $\beta$ s, it is thought that the ECM defects arising from the absence of *ADAMTSL2* lead to TGF $\beta$  dysregulation. Excess TGF $\beta$  activity is thought to lead to fibroblast-myofibroblast transition.<sup>10,11</sup> A potential link to altered TGF $\beta$  signaling is also strengthened by finding *LTBP3* mutations in GD.<sup>12</sup>

GD type 1 is a progressive disorder in which affected individuals have a short stature, brachydactyly, thick skin, restricted joint mobility, and a "happy" face due to characteristic facial features.<sup>5,13-16</sup> The name geleophysic dysplasia comes from the Greek words *geleos*, meaning "happy" and *physis*, meaning "nature." Other findings in individuals with GD can include hepatomegaly, tracheal stenosis, pseudomuscular hypertrophy (due to excessive collagen), and cardiac disease characterized by thickening of mitral, pulmonary, and aortic valves.<sup>5,13-16</sup> The cardiac and tracheal

**Table 1.** Clinical features of *ADAMTSL2* mutations reported in dogs, humans, and mice.

Clinical Features	Dog ( <i>ADAMTSL2</i> mutation)	Human ( <i>ADAMTSL2</i> mutation)	Mouse ( <i>Adamtsl2</i> deletion)
Joint stiffness	2/2	Yes	Not seen <sup>a</sup>
Ear fold	2/2	No	Not seen <sup>a</sup>
Short stature	2/2	Yes	Not seen <sup>a,b</sup>
Pulmonary airway abnormalities	0/2	Yes	Yes
Cardiac abnormalities	2/2	Yes	Yes
Seizures	1/2	No	Not seen <sup>a</sup>
Wide-set eyes	2/2	Y; with narrowed palpebral fissures	Not seen <sup>a</sup>
Broad muzzle/nose	2/2	Yes	Not seen <sup>a</sup>
Brachydactyly	2/2	Yes	Not seen <sup>a,b</sup>
Pseudomuscle hypertrophy	2/2	Yes	Not seen <sup>a</sup>
Pleasant disposition	2/2	Yes	NA
Other organ dysfunction	0/2; dense collagen around organs	Yes	Not seen <sup>a</sup>
Bone replaced by fibrous tissue	1/1 (only 1 dog evaluated)	No; delayed age of long bones, cone-shaped epiphysis	Not seen <sup>a</sup>
Thick skin	1/1 (only 1 dog evaluated)	Yes	Not seen <sup>a</sup>
Fatality rate	Unknown; appears to stabilize	33% fatality rate by 5 years	Lethal mutation

<sup>a</sup>Mice with *Adamtsl2* deletion die shortly after birth. The anomalies were not seen in newborn mutant mice, but may possibly appear with maturity.

<sup>b</sup>Conditional deletion of *Adamtsl2* in limbs leads to shorter limb bones and brachydactyly (Hubmacher D, Apte, S.S., unpublished data).

abnormalities of GD lead to death in 33% of affected individuals before the age of 5.<sup>14</sup>

The Beagles described in this report exhibited a similar array of features (Table 1), including brachydactyly of the outer digits, broad facial features including wide-set eyes, a characteristic ear fold, fibrosis of the joints, and a pleasant disposition. The fibrosis of joint capsules leads to their characteristic “tiptoe” gait, and skin fibrosis leads to the wide-set eyes and broad muzzle. Some owners report that the skin is tight, which was not apparent in these cases. Cardiac disease has been inconsistently reported in association with MLS.<sup>17</sup> Seizures have also been reported in other affected Beagles with this disease, which is consistent with Case 1, but no underlying etiology has been identified in the literature.<sup>2,17</sup> In contrast to humans with GD in which the disease progresses rapidly, Beagles with MLS appear to stabilize at about 1 year of age and have a normal life span unless other congenital defects are present.<sup>17</sup>

Of interest, the endomysial and perimysial connective tissue layers of muscle appeared to be preserved, whereas the epimysial layer surrounding the entire muscle was thickened. It is not clear whether collagen types differ between different connective tissue layers in muscle. Another possibility is selective expression and functional association of *ADAMTSL2* with the epimysial cells. There were both clinical evidence and pathological confirmation of thickened skin in Case 2. Although a duplicate screen of collagen VI, fibrillins, and laminin- $\alpha$ 2 was not performed on skin as they were on muscle, extensive fibrosis (ie, accumulation of collagen) was documented on routine postmortem examination in Case 2.<sup>2</sup> In the *Adamtsl2* knockout mouse, the bronchial epithelial cells appear to be most severely affected, with muscle generally preserved or only mildly affected.<sup>7</sup> This species difference could arise from the inability of affected mice to survive past birth, which could mask a progressive muscle or skin disorder, or to differences in the fibrillin repertoire of these species, because humans and dogs have 3 fibrillins, but mice only have 2 fibrillins.<sup>18</sup> *ADAMTSL2* is thought to selectively influence assembly of fibrillin-1, and fibrillin-2, or both through direct binding, and analysis of *Adamtsl2*-/- mice demonstrated an excess of fibrillin-2 microfibrils in the bronchii.<sup>7,10</sup> The variable phenotypic manifestation in different tissues could also depend on different fibrillin-1/fibrillin-2 ratios in specific tissues, and the degree to which other ADAMTS proteins may be able to compensate,<sup>6,10</sup> which then determine the effect of the *ADAMTSL2* mutation.<sup>7</sup> In this context, little is presently known about ADAMTS proteins and fibrillins in canine tissues and during canine development. Investigating this could be a complex undertaking, because in mice, for example, *Adamtsl2* mRNA shows a dynamic expression pattern and was detected in developing skeletal muscle, as well as liver, bronchial and arterial smooth muscle, skin, nucleus pulposus of the intervertebral disk, perichondrium, pancreas, and spinal cord.<sup>7,19</sup>

Analysis of dermal fibroblasts from MLS dogs was necessarily limited and should be considered preliminary

because of the lack of sufficient number of cells and of strain- and appropriate age-matched controls. Nevertheless, the findings are consistent with previous work demonstrating the increase in soluble TGF $\beta$  and strongly suggesting myofibroblastic transition of the MLS fibroblasts, represented by strong SMA expression, and enhanced contractility within collagen gels.<sup>4,20</sup> In summary, the present study expands on the clinical understanding of MLS, provides additional tissue analysis, and limited cell analysis which supports a potential profibrotic effect of the MLS mutation and a physiological antifibrotic role for *ADAMTSL2* in some tissues such as muscle and skin.

### Site of work

The clinical work was performed at the Purdue University Veterinary Teaching Hospital and the University of Missouri Veterinary Medical Teaching Hospital. Laboratory studies were performed at the Cleveland Clinic Lerner Research Institute and the Comparative Neuromuscular Laboratory, School of Medicine, University of California San Diego.

### Funding

The work was supported in part by NIH awards AR53890 (to SA) and T32HL007914-08 to HB (Training Program in Vascular Biology and Pathology, Principal Investigator, Edward Plow).

### Prior Submission

This manuscript has not been submitted elsewhere. A synopsis of the clinical findings in the dogs described in this study was previously published in a manuscript identifying the genetic basis of Musladin-Lueke syndrome (Bader et al., PLoS One 2010 Sep 17;5(9):pii: e12817, supplemental text). This manuscript here presents a complete clinical description of the cases as well as previously unpublished laboratory research using tissue and cells from the cases.

*Conflict of Interest Declaration:* Authors declare no conflict of interest.

*Off-label Antimicrobial Declaration:* Authors declare no off-label use of antimicrobials.

### References

1. Buchanan JW, Bucheler J. Vertebral scale system to measure canine heart size in radiographs. *J Am Vet Med Assoc* 1995;206:194–199.
2. Bader HL, Ruhe AL, Wang LW, et al. An *ADAMTSL2* founder mutation causes musladin-lueke syndrome, a heritable disorder of beagle dogs, featuring stiff skin and joint contractures. *PLoS ONE* 2010;5:e12817.
3. Hattori N, Carrino DA, Lauer ME, et al. Pericellular versican regulates the fibroblast-myofibroblast transition: A role for ADAMTS5 protease-mediated proteolysis. *J Biol Chem* 2011;286:34298–34310.
4. Le Goff C, Morice-Picard F, Dagonneau N, et al. *ADAMTSL2* mutations in geleophysic dysplasia demonstrate a

role for ADAMTS-like proteins in TGF-beta bioavailability regulation. *Nat Genet* 2008;40:1119–1123.

5. Allali S, Le Goff C, Pressac-Diebold I, et al. Molecular screening of ADAMTSL2 gene in 33 patients reveals the genetic heterogeneity of geleophysic dysplasia. *J Med Genet* 2011;48:417–421.

6. Le Goff C, Mahaut C, Wang LW, et al. Mutations in the TGFbeta binding-protein-like domain 5 of FBN1 are responsible for acromicric and geleophysic dysplasias. *Am J Hum Genet* 2011;89:7–14.

7. Hubmacher D, Wang LW, Mecham RP, et al. Adamtsl2 deletion results in bronchial fibrillin microfibril accumulation and bronchial epithelial dysplasia: A novel mouse model providing insights on geleophysic dysplasia. *Dis Model Mech* 2015;8:487–499.

8. Bona CA, Murai C, Casares S, et al. Structure of the mutant fibrillin-1 gene in the tight skin (TSK) mouse. *DNA Res* 1997;4:267–271.

9. Hubmacher D, Apte SS. ADAMTS proteins as modulators of microfibril formation and function. *Matrix Biol* 2015;47:34–43.

10. Hubmacher D, Apte SS. Genetic and functional linkage between ADAMTS superfamily proteins and fibrillin-1: A novel mechanism influencing microfibril assembly and function. *Cell Mol Life Sci* 2011;68:3137–3148.

11. Le Goff C, Cormier-Daire V. From tall to short: The role of TGFbeta signaling in growth and its disorders. *Am J Med Genet C Semin Med Genet* 2012;160c:145–153.

12. McInerney-Leo AM, Le Goff C, Leo PJ, et al. Mutations in LTBP3 cause acromicric dysplasia and geleophysic dysplasia. *J Med Genet* 2016;53:457–464.

13. Spranger JW, Gilbert EF, Tuffli GA, et al. Geleophysic dwarfism—a “focal” mucopolysaccharidosis? *Lancet* 1971;2:97–98.

14. Pontz BF, Stoss H, Henschke F, et al. Clinical and ultrastructural findings in three patients with geleophysic dysplasia. *Am J Med Genet* 1996;63:50–54.

15. Le Goff C, Cormier-Daire V. Geleophysic Dysplasia. In: Pagon RA, Adam MP, Ardinger HH, Wallace SE, Amemiya A, Bean LJH, Bird TD, Fong CT, Mefford HC, Smith RJH, Stephens K, eds. *GeneReviews(R)*. Seattle (WA): University of Washington; 1993-2017. 2009 Sep 22 [updated 2012 Apr 19].

16. Shohat M, Gruber HE, Pagon RA, et al. Geleophysic dysplasia: A storage disorder affecting the skin, bone, liver, heart, and trachea. *J Pediatr* 1990;117:227–232.

17. Musladin JM, Musladin AM, Lueke A. Your Beagle's Health and Genetics. In: Musladin JM, Musladin AM, Lueke A, eds. *The New Beagle: A Dog for All Seasons*, 2nd ed. New York: Macmillan General Reference; 1998:202–206.

18. Hubmacher D, Tiedemann K, Reinhardt DP. Fibrillins: From biogenesis of microfibrils to signaling functions. *Curr Top Dev Biol* 2006;75:93–123.

19. Koo BH, Le Goff C, Jungers KA, et al. ADAMTS-like 2 (ADAMTSL2) is a secreted glycoprotein that is widely expressed during mouse embryogenesis and is regulated during skeletal myogenesis. *Matrix Biol* 2007;26:431–441.

20. Hinz B, Gabbiani G. Cell-matrix and cell-cell contacts of myofibroblasts: Role in connective tissue remodeling. *Thromb Haemost* 2003;90:993–1002.